JOURNAL OF BACTERIOLOGY, June 2002, p. 2914–2924 Vol. 184, No. 11
0021-9193/02/$04.00+0 DOI: 10.1128/JB.184.11.2914–2924.2002

Identification and Physical Characterization of the HbpR Binding Sites of the *hbpC* and *hbpD* Promoters

David Tropel and Jan Roelof van der Meer*

Process of Environmental Microbiology and Molecular Ecotoxicology, Swiss Federal Institute for Environmental Science and Technology (EAWAG), CH-8600 Dübendorf, Switzerland

Received 17 October 2001/Accepted 24 February 2002

Pseudomonas azelaica **HBP1 can use 2-hydroxybiphenyl (2-HBP) and 2,2′-dihydroxybiphenyl as sole carbon and energy sources by means of the *hbp* regulon. This regulon is composed of three genes, *hbpCA* and *hbpD*, coding for enzymes of a *meta*-cleavage pathway and the *hbpR* gene, which codes for a XylR/DmpR-type transcription regulator. It was previously shown that HbpR activates transcription from two σ^{54}-dependent promoters, P_{hbpC} and P_{hbpD}, in the presence of 2-HBP. In this study, by using gel mobility shift assays with a purified fusion protein containing calmodulin binding protein (CBP) and HbpR, we detected two binding regions for HbpR in P_{hbpC} and one binding region in P_{hbpD}. DNase I footprints of the proximal binding region of P_{hbpC} and of the binding region in P_{hbpD} showed that CBP-HbpR protected a region composed of two inverted repeat sequences which were homologous to the binding sites identified for XylR. Unlike the situation in the XylR/P_u system, we observed simultaneous binding of CBP-HbpR on the two upstream activating sequences (UASs). Fragments with only one UAS did not show an interaction with HbpR, indicating that both pairs of UASs are needed for HbpR binding. The addition of both ATP and 2-HBP increased the DNA binding affinity of HbpR. These results showed for the first time that, for regulators of the XylR/DmpR type, the effector positively affects the recruitment of the regulatory protein on the enhancer DNA.**

Pseudomonas azelaica HBP1 metabolizes 2-hydroxybiphenyl (2-HBP) and 2,2′-dihydroxybiphenyl through a *meta*-cleavage pathway (14, 15, 29). The enzymes involved in the first degradation steps are encoded by the *hbpCA* and *hbpD* genes (Fig. 1). Two promoters, designated P_{hbpC} and P_{hbpD} (13), control the expression of the *hbpCA* and *hbpD* genes, respectively. In the presence of 2-HBP, transcriptional activation from both promoters is mediated by the HbpR regulatory protein (11). On the basis of sequence similarities, HbpR has been identified as a member of the XylR/DmpR subclass of the NtrC family of prokaryotic enhancer binding proteins. Proteins of this family activate transcription at a distance from their cognate promoter through an intrinsic ATPase activity in concert with RNA polymerase containing the alternative sigma factor σ^{54} (6, 10). The process of activation by proteins of the XylR/DmpR subclass is initiated by a direct interaction with aromatic compounds which (mostly) are the substrates for the pathways to be controlled (32). It has been shown that for proper activation, the regulatory protein needs to bind at specific nucleotide sequences in its cognate promoter. These sequences are formed by two (imperfect) palindromic sequences of approximately 16 bp and with a spacing of 29 to 42 bp between the centers of the palindromes. They are usually called bacterial enhancer-like elements or upstream activating sequences (UASs) and are located 100 to 200 bp upstream of the −12/−24 target promoter (17, 20). This distance does not allow direct contact between the regulator and the σ^{54} RNA polymerase; therefore, looping of the DNA is required, bringing together both partners. Looping is facilitated by induced bending of the DNA by integration host factor or HU or by intrinsically curved DNA sequences (21). Changing the relative positions of the −12/−24 motif, the integration host factor binding site, and the UASs was shown to disturb the optimal promoter geometry and to lead to a decrease in transcriptional activation (1, 2, 8, 9, 20).

Proteins of the NtrC family have an intrinsic binding affinity for their UASs. In the absence of an effector (for regulators of the XylR type) or phosphorylation (for NtrC-type regulators), two dimers of the regulatory protein bind to the UASs (22, 26, 30). In contrast, the activated regulatory protein (for NtrC, its phosphorylated form) forms larger protein complexes at the UAS DNA. The latter finding was determined by atomic force microscopy and analytical ultracentrifugation, which showed that phosphorylated NtrC in the presence of the UAS DNA oligomerizes to the size of hexamers or octamers (26, 37). This oligomerization is a requirement for transcriptional activation. Although some conflicting data exist on this topic, binding of the dimers in the inactive state to each of the UASs in the native *glnA* promoter occurs with different affinities (22). Upon activation of the regulatory protein, the differences in the binding affinities for each of the UASs increase strongly (25, 31). In the current activation model, it is assumed that there is continuous cycling among the inactive dimer in solution, the inactive two-dimer pair on the UAS DNA, and the octameric (active) complex (7). XylR itself is supposed to follow more or less the same model as NtrC, except that activation of the protein takes place through effector binding and not through phosphorylation. However, most of the studies on XylR binding and activation have been made with a protein with a deletion of its N-terminal effector binding domain (ΔAXylR) (18–20). Since this protein is constitutively active, the exact changes

* Corresponding author. Mailing address: Process of Environmental Microbiology and Molecular Ecotoxicology, Swiss Federal Institute for Environmental Science and Technology (EAWAG), Postbox 611, CH-8600 Dübendorf, Switzerland. Phone: 41 1 823 54 38. Fax: 41 1 823 5547. E-mail: vdmeer@eawag.ch.

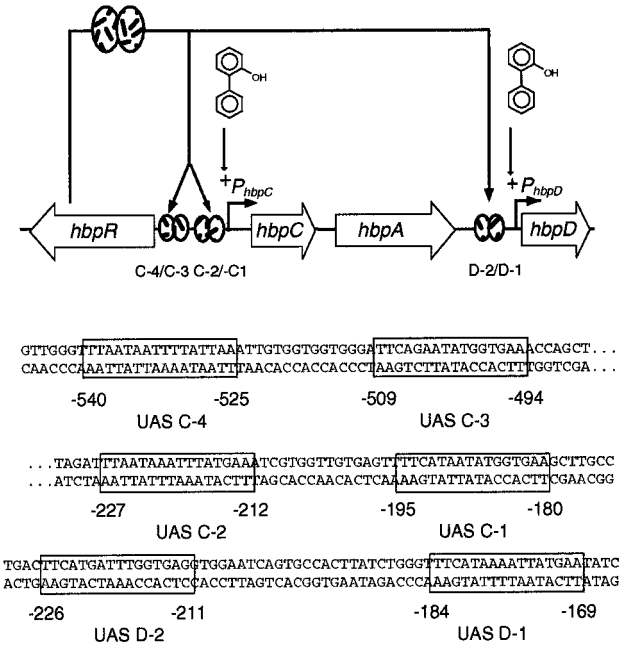

FIG. 1. Genetic organization of the *hbp* genes in *P. azelaica* HBP1. Arrows depict the orientations and sizes of the genes; the solid line indicates noncoding DNA. The *hbpR* gene codes for the regulatory protein, which activates transcription from the *hbpC* and *hbpD* promoters upon exposure to 2-HBP. Regions containing the binding sites for HbpR (UAS) are shown within boxes in the sequence. Sequence numbers refer to the locations of the transcriptional start sites of *hbpC* and *hbpD*.

in DNA binding affinity upon effector binding could not be shown directly.

The HbpR regulatory system has already demonstrated several differences with respect to the DmpR/P_o and XylR/P_u systems. First, the HbpR protein has only 40% amino acid similarity with XylR and DmpR, whereas XylR and DmpR share 67% similar amino acids (13). Second, HbpR is the only member of the XylR/DmpR subclass described so far which is activated by biaromatic compounds, such as 2-HBP and 2,2′-dihydroxybiphenyl. Third, HbpR activates transcription from two promoters within a rather small cluster of only three genes (*hbpCA* and *hbpD*), an unusual scenario (11). Finally, the proposed binding sites for HbpR have slightly larger spacing between the UASs (13). Because of these differences, we were interested in investigating whether the interaction of HbpR with its binding regions also distinguishes it from the other members of the XylR/DmpR subclass. Furthermore, rather than working with an HbpR protein containing an N-terminal A-domain deletion (like most of the DNA binding studies with DmpR and XylR), our goal was to determine the DNA binding characteristics for the entire protein. For this purpose, we set out to produce and purify a fusion protein consisting of calmodulin binding protein (CBP) fused to the N terminus of HbpR (CBP-HbpR). This purified protein was used to study the initial interactions of HbpR on its cognate binding sites in the presence and absence of either ATP or 2-HBP. The characteristics of binding of HbpR to the three pairs of UASs were assessed by using DNase I footprinting and gel mobility shift assays (GMSAs). Our data indicate that HbpR binds simultaneously to both palindromic sequences and that both palindromes are required for HbpR binding. An increase in DNA binding affinity was observed in the presence of 2-HBP and ATP.

MATERIALS AND METHODS

Strains and medium. *Escherichia coli* DH5α (27) was used as a host strain in routine cloning experiments. *E. coli* BL21(DE3)(pLysS) (Stratagene, La Jolla, Calif.) was used for protein overexpression. *E. coli* strains were grown at 25, 30, or 37°C on Luria-Bertani (LB) medium (27). When required, the medium was supplemented with the following antibiotics at the indicated concentrations: ampicillin, 100 $\mu g \cdot ml^{-1}$, and chloramphenicol, 25 $\mu g \cdot ml^{-1}$. All strains and plasmids used in this study are listed in Table 1.

Recombinant DNA techniques. DNA sequencing, plasmid DNA isolation, ligation, transformation, and other DNA manipulations were carried out according to well-established procedures (27). Restriction endonucleases and other DNA-modifying enzymes were obtained from Amersham International plc (Little Chalfont, United Kingdom), Roche Biochemicals (Mannheim, Germany), and New England Biolabs Inc. (Beverly, Mass.) and used according to the specifications of the manufacturers. DNA fragments were isolated from agarose gels by using a PEQLAB kit (Biotechnologie GmbH, Erlangen, Germany). Double-stranded template sequencing on plasmids was performed by using a modified dideoxy-chain termination method (28) with primers that were labeled with the fluorescent dye IRD-800 at the 5′ end as described elsewhere (23).

Cloning of the *hbpR* overexpression vector. Plasmid pCAL-n-FLAG (Stratagene) was used for the production and purification of the HbpR protein in *E. coli*. To clone *hbpR* into pCAL-n-FLAG, its first 494 nucleotides were amplified by using PCR with plasmid pHBP130 and primers LIChbpR1 (5′-GACGACG ACAAGATGAAATCAAATAAAAATAATAG) and LIChbpR2 (5′-GGAAC AAGACCCGTTACGCAACGGAAAACCAA). The PCR product was separated on an agarose gel, purified, and treated with *Pfu* polymerase (Stratagene) in the presence of dATP. The 3′-5′ exonuclease activity of *Pfu* polymerase removes nucleotide residues from both 3′ ends of the PCR product and stops on the first adenine residue because of the dATP present in the reaction. Thereby, 5′ single-stranded overhangs were generated (5′-GACGACGACAAGAT and 5′-GGAACAAGACCCGT) that were complementary to those in the prepared vector. Next, the *hbpR* fragment was ligated with pCAL-n-FLAG according to the manufacturer's recommendations. Transformation resulted in plasmid pHB150. The complete *hbpR* gene was assembled as follows: a 1.475-kb *Nsi*I-*Sal*I fragment from pHYBP132 containing the remaining sequence of *hbpR* was used to replace a 65-bp fragment of pHB150 cut with *Nsi*I and *Sal*I (yielding pHB151). Plasmid pHB151 produced an HbpR protein with an N-terminal CBP tag.

Overexpression and purification of CBP-HbpR. *E. coli* BL21(DE3)(pLysS) containing pHB151 was grown at 30°C in LB medium to an optical density at 600 nm of 0.6. To induce T7 RNA polymerase-directed expression, isopropyl-β-D-1-thiogalactopyranoside (IPTG) was added at a concentration of 0.1 mM, and cultures were further incubated for 3 h at 25°C. Bacteria were collected from 1 liter of culture, washed in 50 mM Tris-HCl buffer (pH 7.5), and centrifuged. After the supernatant was discarded, the cell pellet was stored frozen at −80°C. To disrupt cells, the bacterial pellet was thawed in 15 ml of loading buffer (loading buffer is 50 mM Tris-HCl, 1 mM magnesium acetate, 1 mM imidazole, 2 mM $CaCl_2$, and 10% [vol/vol] glycerol [pH 8.0]) containing 400 mM NaCl and then subjected to ultrasonication four times for 1 min each time at 50% and 40 W (Branson 450 Sonifier). All subsequent steps were carried out at 4°C. The cell extract obtained was centrifuged for 30 min at 35,000 × *g* to remove cell debris. The supernatant was loaded on a 3-ml column of calmodulin resin equilibrated with loading buffer. After loading, the column was washed with 20 bed volumes of loading buffer containing 400 mM NaCl and then with 10 bed volumes of loading buffer containing 150 mM NaCl. Proteins binding to calmodulin were removed with elution buffer (elution buffer is 50 mM Tris-HCl, 0.2 mM EGTA, 150 mM NaCl, and 10% [vol/vol] glycerol [pH 8.0]). Fractions eluted from the column were collected in 1-ml portions and frozen in 30-μl aliquots at −80°C. The method of Bradford was used to determine the total protein concentration in our samples. Protein samples were analyzed by sodium dodecyl sulfate (SDS)-polyacrylamide gel electrophoresis (PAGE), and the intensities of the different bands were quantified by laser densitometry scanning (300S computing densitometer; Molecular Dynamics, Sunnyvale, Calif.) by using the program ImageQuant (Molecular Dynamics). The proportion of CBP-HbpR was determined as the band intensity relative to the intensity of all bands. From the proportion and the total protein concentration, the concentration of CBP-HbpR was calculated.

TABLE 1. Strains and plasmids used in this study

Strain or plasmid	Relevant genotype or characteristics	Source or reference
E. coli strains		
DH5α	*endA1 hsdR17* (r_K^- m_K^-) *supE44 thi-1 recA1 gyrA96 relA1* F^- Δ(*argF-lacZYA*)*U169* (ϕ80d*lacZ*Δ*M15*)λ^-	Gibco BRL
BL21(DE3)(pLysS)	*ompT lon hsdSB* (r_B^- m_B^-) *gal dcm* (DE3) pLysS Cm^r	Stratagene
Plasmids		
pGEM-T-Easy	Ap^r	Promega
pCAL-n-FLAG	Ap^r; expression vector	Stratagene
pHBP130	Ap^r ColE1; contains a 7.8-kb *Mlu*I-*Sal*I fragment from *P. azelaica* HBP1 with *hbpR* and *hpbC*	(29)
pHYBP109	Ap^r ColE1; pJAMA8 carrying *hbpR* under the control of its native promoter (P_{hbpR})	(13)
pHYBP132	Ap^r ColE1; pET3d containing *hbpR* under the control of the ϕ10 promoter	(13)
pJAMA8	Ap^r ColE1; *luxAB*-based promoter-probe vector	(13)
pHB150	Ap^r; pCAL-n-EK vector Stratagene carrying the 0.5-kb PCR fragment containing the start of *hbpR*	This study
pHB151	Ap^r; pHB150 carrying the 1.5-kb *Nsi*I-*Sal*I fragment from pHYBP132 which generated a complete *hbpR*	This study
pHB152	pGEM-T-Easy containing a 117-bp fragment with UAS C-2 obtained by PCR with primers hbpC11 and hbpC12	This study
pHB153	pGEM-T-Easy containing an 85-bp fragment obtained by PCR with primers hbpC11 and hbpC15	This study
pHB154	pGEM-T-Easy containing an 86-bp fragment obtained by PCR with primers hbpC10 and hbpC13	This study
pHB155	pGEM-T-Easy containing a 118-bp fragment with UAS C-1 obtained by PCR with primers hbpC10 and hbpC14	This study
pHB156	pHB152 containing a 450-bp *Nae*I-*Bam*HI fragment from pHB154; contains only UAS C-2	This study
pHB157	pHB153 containing a 480-bp *Nae*I-*Bam*HI fragment from pHB155; contains only UAS C-1	This study
pHB158	pGEM-T-Easy containing a 118-bp fragment with UAS C-2 obtained by PCR with primers hbpC11 and hbpC16	This study
pHB160	pGEM-T-Easy containing a 110-bp fragment with UAS C-1 obtained by PCR with primers hbpC10 and hbpC17	This study
pHB161	pGEM-T-Easy containing a 115-bp fragment with UAS C-1 obtained by PCR with primers hbpC10 and hbpC18	This study
pHB162	pHB158 containing the 470-bp *Nae*I-*Bam*HI fragment from pHB160 with UAS C-1; contains UASs C-1 and C-2 + 5 bp	This study
pHB163	pHB158 containing the 475-bp *Nae*I-*Bam*HI fragment from pHB161 with UAS C-1; contains UASs C-1 and C-2 + 10 bp	This study
pHB164	pHB151 containing a 2.75-kb *Bam*HI fragment from pHB109 with an *hbpR-hbpC* intergenic region–*luxAB* fusion; complete *cbp-hbpR*	This study
pHB165	pHB150 containing a 2.75-kb *Bam*HI fragment from pHB109 with an *hbpR-hbpC* intergenic region–*luxAB* fusion; incomplete *cbp-hbpR*	This study
pHB207	Ap^r; pHB150 carrying the 2-kb *Bgl*II-*Sal*I fragment from pHYBP132 which generated a complete *hbpR* without the CBP tag fusion	This study
pHB208	pHB207 containing a 2.75-kb *Bam*HI fragment from pHB109 with an *hbpR-hbpC* intergenic region–*luxAB* fusion; complete *hbpR*	This study

Construction of plasmids for DNA binding studies. Various DNA fragments were generated by using PCR in order to determine the locations of the HbpR binding regions. The sequences and locations of the primers used for this step are listed in Table 2. Furthermore, the UAS C-1 and C-2 regions were modified by deleting either one of the UASs or adding additional nucleotides between the two UASs. This step was also performed by using PCR (Table 2). For example, to remove the proximal site (UAS C-1), primers hbpC11 and hbpC12 were used. This step amplified a fragment with only the distal site (UAS C-2). Primers hbpC10 and hbpC13 were used to amplify the region downstream of UAS C-1. Both PCR fragments were separately cloned in pGEM-T-Easy to give pHB152 and pHB154, respectively. The amplified sequence was recovered from pHB154 as an *Nae*I-*Bam*HI fragment and inserted into pHB152 (yielding pHB156). Using the same strategy, we constructed plasmids pHB157, pHB162, and pHB163, which contained a binding region with a deletion of UAS C-2, a binding region with 5 bp inserted between the UASs, and a binding region with 10 bp inserted between the UASs, respectively.

DNase I footprinting. The DNA fragments used for DNase I footprinting were amplified by PCR. For each PCR, one oligonucleotide was end labeled by phosphorylation with [γ-^{32}P]ATP, allowing the specific labeling of one strand. The end-labeled fragments were mixed with various amounts of HbpR (0 to 450 nM) in binding buffer (binding buffer is 10 mM Tris-HCl, 20 mM KCl, 1 mM EDTA, and 10% [vol/vol] glycerol), to which 1 μg of poly(dI-dC) was added. DNA-protein complexes were allowed to form at 33°C for 15 min in a total volume of 50 μl for each footprinting reaction. DNase I (0.05 U; Roche Biochemicals) was then added to the reaction mixture, as were 1 mM $MgCl_2$ and 0.5 mM $CaCl_2$. The reaction mixture was incubated for 1 min at 30°C, and the reaction was stopped by the addition of 140 μl of stop mix solution (stop mix solution is 770 mM sodium acetate, 130 mM EDTA, and 256 μg of yeast tRNA ml^{-1}). The footprinting mixture was subsequently extracted once with phenol and chloroform (1:1 [vol/vol]) and once with chloroform, and finally the DNA was precipitated with ethanol. The DNA was washed once with 70% ethanol, dried, resuspended in 5 μl of sequence loading buffer (sequence loading buffer is deionized formamide containing 10 mM EDTA, 0.3% [wt/vol] bromophenol blue, and 0.3% xylene cyanol), and loaded on a 6% polyacrylamide gel which contained 8 M urea and which had been prerun for 1 h. The gel was run at 1,800 V for 3 h in Tris-borate-EDTA (TBE) buffer (27). As size markers, DNA

TABLE 2. Primers used in this study

Primer	Nucleotide sequence[a]	Position from the 5′ end[b]
LIChbpR1	5′-GACGACGACAAGATGAAATCAAATAAAAATAATAG	*hbpR* start codon
LIChbpR2	5′-GGAACAAGACCCGTTACGCAACGGAAAACCAA	494 bp downstream of *hbpR* start codon
hbpC2	5′-CTGGCTAGGCGACAGCC	459 bp upstream of *hbpC* start codon
hbpC4	5′-CCTGGCATGAGCTATCA	322 bp upstream of *hbpC* start codon
hbpC6	5′-AATGAGCGCCAGAAAGCCT	156 bp upstream of *hbpC* start codon
hbpC8	5′-TACCCGAGATTTGAAATCATTG	20 bp downstream of *hbpC* start codon
hbpCA	5′-ATTTTTATTTGATTTCATGGCGA	672 bp upstream of *hbpC* start codon
hbpCB	5′-GGCATCTGCCGACGGATC	534 bp upstream of *hbpC* start codon
hbpCC	5′-AACGATGGTGCGGTTTTCAT	385 bp upstream of *hbpC* start codon
hbpCD	5′-GACCGCGGAAGGGGTTTAC	206 bp upstream of *hbpC* start codon
hbpC10	5′-CGGG*CATATG*GCGCCAGAAAGCCTAGCTCC	162 bp upstream of *hbpC* start codon
hbpC11	5′-CGGG*AAGCTT*TGGTGCGGTTTTCATGGTCCTTA	390 bp upstream of *hbpC* start codon
hbpC12	5′-CGCG*GGATCC*AACTCACAACCACGATTTCATAAA	264 bp upstream of *hbpC* start codon
hbpC13	5′-CGCG*GGATCC*GCTTGCCCGCCATGGCAAG	248 bp upstream of *hbpC* start codon
hbpC14	5′-CGCG*GGATCC*ATCGTGGTTGTGAGTTTTCATAATA	280 bp upstream of *hbpC* start codon
hbpC15	5′-CGCG*GGATCC*ATCTACGAGAACCCTATCTATCTACTC	296 bp upstream of *hbpC* start codon
hbpC16	5′-CGCG*GGATCC*CCACGATTTCATAAATTTATTAAATC	273 bp upstream of *hbpC* start codon
hbpC17	5′-CGCG*GGATCC*TGTGAGTTTTCATAATATGGTGAAG	271 bp upstream of *hbpC* start codon
hbpC18	5′-CGCG*GGATCC*GTGGTTGTGAGTTTTCATAATATG	276 bp upstream of *hbpC* start codon
hbpD1	5′-CATCCTTGGGAGGGCGTAAC	850 bp upstream of *hbpD* start codon
hbpD2	5′-CTTCAGAGCACTCGCCAC	561 bp upstream of *hbpD* start codon
hbpD3	5′-TGGATCTGCAGTTGCCCTAAG	622 bp upstream of *hbpD* start codon
hbpD4	5′-ATGAAGAGCGCGCGCGCTCTC	366 bp upstream of *hbpD* start codon
hbpD5	5′-GCATTCCTCCTCCAGATGAG	423 bp upstream of *hbpD* start codon
hbpD8	5′-CAGTGTACTTTGGCATTGGTC	15 bp downstream of *hbpD* start codon

[a] Restriction sites for *Bam*HI (5′-GGATCC-3′), *Nde*I (5′-CATATG-3′), and *Hin*dIII (5′-AAGCTT-3′) are shown in italic type. Mismatched residues at the 5′ end which resulted from the introduction of restriction or ligation-independent cloning overhangs are underlined.

[b] When there were mismatches at the 5′ ends, the position of the residue downstream of the first mismatch is given.

fragments which had been generated in a dideoxy sequencing reaction (28) with a Sequenase (version 2.0) DNA sequencing kit (Amersham) were loaded. After the run, the gel was soaked in a solution of 10% acetic acid, dried, and exposed overnight to Biomax film (Kodak) at −80°C.

GMSAs. For GMSAs, the ^{32}P-end-labeled fragments and the binding buffer were the same as those used in the footprinting assays. The reaction volume was reduced to 30 μl. When tested, 2-HBP and ATP were added to the reaction mixture at 10 and 5 mM, respectively. After binding, 5 μl of GMSA loading buffer (GMSA loading buffer is 40% glycerol [vol/vol], 50 mM EDTA, 0.1% [wt/vol] bromophenol blue, and four-times-concentrated TBE buffer) was added, and the mixture was loaded on a 5% polyacrylamide gel in TBE buffer. Separation was done for 2 h at 50 V in a Mini-Protean vertical electrophoresis chamber (Bio-Rad). The gel was dried and exposed overnight to Kodak X-Omat film at −80°C. Autoradiograms of GMSAs were quantitatively analyzed by densitometric scanning. Relative densities were calculated by comparing the measured densities of shifted bands to that in the lane in which CBP-HbpR had completely bound all DNA.

In vivo HbpR activation. To determine the in vivo activity of the CBP-HbpR fusion protein, we used HbpR-mediated activation of the *luxAB* genes transcriptionally fused to the *hbpC* promoter as described before (11). The CBP-HbpR fusion of pHB151 was completed with the 2.75-kb *Bam*HI fragment of plasmid pHYBP109 (containing the native *hbpRC* intergenic region fused to the *luxAB* genes). This *Bam*HI fragment was inserted at the single *Bgl*II site of plasmid pHB151. After transformation, plasmids in which *cbp-hbpR* was expressed from the native *hbpR* promoter were selected (yielding pHB164). Similarly, pHB165 was constructed starting with pHB150. In plasmid pHB165, the *hbpR* gene has a deletion in the region coding for the C-terminal portion of the protein. This plasmid served as a negative control for 2-HBP-dependent luciferase activation. As a positive control, the *hbpR* gene was cloned under the control of the T7 gene ϕ10 promoter but without the CBP tag fusion. *hbpR* was cloned as a 2-kb *Bgl*II -*Sal*I fragment of plasmid pHB132 and inserted into pHB150 cut with the same enzymes (yielding plasmid pHB207). Plasmid pHB207 was completed with the 2.75-kb *Bam*HI fragment of plasmid pHYBP109 (yielding pHB208).

Luciferase assays. *E. coli* DH5α with pHB164, pHB165, or pHB208 was induced in 7-ml glass vials that were closed with screw caps with a polytetrafluoroethylene (PTFE) liner (Supelco, Bellefonte, Pa.). The assay mixture contained 1.95 ml of LB medium, 30 μl of *E. coli* culture (at an optical density at 600 nm of 0.45), and 20 μl of dimethyl sulfoxide solution with 2-HBP. The final concentration of 2-HBP in the assay mixture was 25 μM. The negative control contained 20 μl of dimethyl sulfoxide. The glass vials were incubated at 30°C on a rotary shaker at 200 rpm for 2 h. After induction, samples of 0.2 ml were removed and transferred to a microtiter plate. Bioluminescence was measured at 30°C with a final *n*-decanal concentration of 2 mM in a MicroLumat LB 96 P luminometer (Berthold AG, Regensdorf, Switzerland) as described previously (33).

Synthetic oligonucleotides and chemicals. Primers labeled with the fluorescent dye IRD-800 at the 5′ end were purchased from MWG-Biotech GmbH (Ebersberg, Germany). All other primers were obtained from Microsynth GmbH (Balgach, Switzerland). Ultrapure agarose, ammonium persulfate, *N,N,N′,N′*-tetramethylethylenediamine, Tris, and urea were purchased from Life Technologies. Rapid Gel-XL–40% acrylamide solution was obtained from Amersham. IPTG and 5-bromo-4-chloro-3-indolyl-β-D-galactopyranoside (X-Gal) were obtained from Biosynth AG (Staad, Switzerland), and *n*-decanal was obtained from Sigma Chemical Co. (St. Louis, Mo.). Nutrient broth, yeast extract, and tryptic casein were purchased from Biolife S.r.l. (Milan, Italy), and ultrapure agar was obtained from Merck (Darmstadt, Germany). Antibiotics, inorganic salts, and all other organic chemicals were obtained from Fluka AG (Buchs, Switzerland).

RESULTS

Expression and purification of a CBP-HbpR fusion protein. In order to study the characteristics of in vitro binding of HbpR to its DNA binding sites, we decided to express HbpR as a fusion protein in *E. coli* and then purify it. Expression as a fusion protein would most likely not result in its precipitation, a common phenomenon encountered with XylR (5), a protein related to HbpR. A fusion with CBP was chosen, since this choice in principle allowed complete cleavage of CBP from HbpR through an enterokinase cleavage site (36). CBP-HbpR was expressed in *E. coli* at 25°C for 3 h to reduce the formation of insoluble fusion protein observed at 37 or 30°C (data not shown). SDS-PAGE of cell extracts of *E. coli* BL21(pHB151) indeed revealed a protein of 67 kDa, which corresponds to the

molecular mass of HbpR (63 kDa) plus that of CBP (4 kDa). This protein band was not detected in extracts of *E. coli* BL21(pHB150), which produced a truncated protein, CBP-HbpRΔ (Fig. 2A). The CBP-HbpR concentration in the preparation eluted from the calmodulin resin was estimated to be 200 $\mu g \cdot ml^{-1}$. Unfortunately, after binding and elution with calmodulin resin, the CBP-HbpR fusion protein always eluted in the presence of two contaminants, of 60 and 75 kDa (Fig. 2A). These contaminants, however, were also eluted from cell extracts of *E. coli* BL21(pHB150) and *E. coli* BL21, indicating that they were not of HbpR origin. Despite repeated attempts, it was not possible to purify the CBP-HbpR fusion protein from the contaminating proteins by use of the calmodulin resin. Unfortunately, CBP-HbpR was also not stable upon cleavage with enterokinase. We therefore had to use the CBP-HbpR preparation with both contaminants and with a CBP tag in our subsequent studies.

To check for true activity of the CBP-HbpR protein, we always conducted negative control experiments with purified cell extracts from *E. coli* BL21(pHB150), producing CBP-HbpRΔ. Second, we determined whether CBP-HbpR was capable of in vivo activation of the *hbpC* promoter. For this purpose, *E. coli* DH5α containing pHB164 was induced with 25 μM 2-HBP. The luciferase activity detected in *E. coli* expressing the CBP-HbpR fusion protein was similar to that found in *E. coli*(pHB208) expressing the native protein (Fig. 2B). From this result, we concluded that CBP-HbpR protein activates the *hbpC* promoter like the native HbpR protein. In contrast, no inducible expression of luciferase activity was observed in *E. coli* DH5α(pHB165), which expresses a CBP-HbpRΔ fusion protein with only the first 165 amino acids of HbpR (Fig. 2B). This result showed that inducible luciferase expression obtained with *E. coli* DH5α(pHB164) in the presence of 2-HBP was not due to proteins from *E. coli* DH5α itself.

DNA binding of the CBP-HbpR protein. In a previous study, it was shown that HbpR activates transcription from two promoters, P_{hbpC} and P_{hbpD}, localized in the *hbpRC* and *hbpAD* intergenic regions, respectively (11). When tested in GMSAs, the CBP-HbpR purified fraction indeed bound both the *hbpRC* and the *hbpAD* intergenic regions but not the *hbpCA* region, which has no demonstrated HbpR-dependent promoter (data not shown). This result showed that binding to the *hbpRC* and *hbpAD* intergenic regions was specific and confirmed our previous findings that HbpR-dependent promoters were located in these regions. Furthemore, no binding was observed with purified cell extracts from *E. coli* producing CBP-HbpRΔ. This result showed that binding of the *hbpRC* and *hbpAD* intergenic regions was mediated by the CBP-HbpR fusion protein.

To determine the locations of the HbpR binding sites more precisely, a series of overlapping DNA fragments were generated and tested for the ability to be bound by CBP-HbpR (Fig. 3). GMSAs showed that fragments hbpD1D4 and hbpD3D8 (Fig. 3A) retained the ability to be bound by HbpR. These fragments shared a 256-bp region located at positions −359 to −103 with respect to the *hbpD* transcriptional start site. No binding was observed with fragments hbpD1D2 (−587 to −298) and hbpD5D8 (−160 to +278). This result showed that the sequences necessary for binding by HbpR were located between positions −160 and −298 relative to the *hbpD* transcriptional start site. Similarly, the locations of the HbpR binding sites in the *hbpRC* intergenic region were determined with overlapping DNA fragments covering the region between −604 and +76 bp with respect to the *hbpC* transcriptional start site. In this situation, two fragments, namely, hbpCAC2 (−604 to −391) and hbpCCC6 (−317 to −88), were bound by CBP-HbpR. No binding was observed with fragments hbpCBC4 (−468 to −256) and hbpCDC8 (−140 to +86) (Fig. 3B). In contrast to the *hbpD* promoter, therefore, the *hbpC* promoter

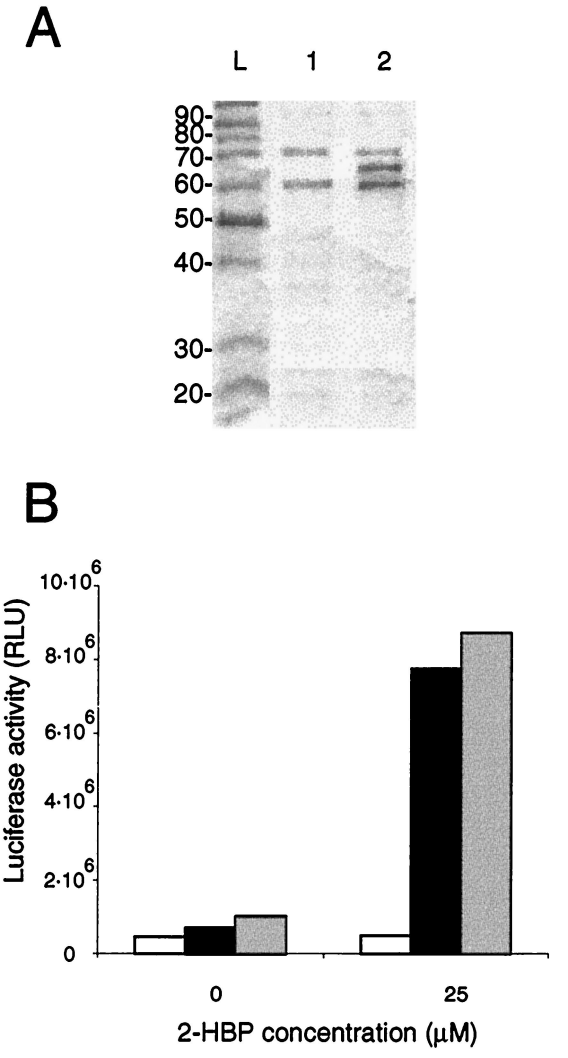

FIG. 2. (A) Analysis by SDS-PAGE of the CBP-HbpR protein fraction after the single calmodulin resin purification step. Lanes: L, protein markers (sizes given in kilodaltons); 1, protein fraction purified from *E. coli* BL21(pHB150), expressing CBP-HbpRΔ; 2, protein fraction purified from *E. coli* BL21(pHB151), expressing CBP-HbpR (67 kDa). The contaminating proteins have sizes of 60 and 75 kDa. (B) Expression of luciferase activity from the *hbpC* promoter of *P. azelaica* reproduced in *E. coli* harboring plasmid pHB164 (black bars) and incubated with 25 μM 2-HBP. Plasmid pHB164 contains the *cbp-hbpR* fusion gene, the *hbpC* promoter, and the *luxAB* genes. As a negative control, *E. coli* harboring plasmid pHB165 (white bars) was used. pHB165 is identical to pHB164, except for a frameshift in *hbpR*. As a positive control, *E. coli* harboring plasmid pHB208 was used (grey bars). pHB208 is identical to pHB164, except that it contains the native *hbpR* gene. Luciferase activity was measured after 2 h of induction at 37°C. RLU, relative light units.

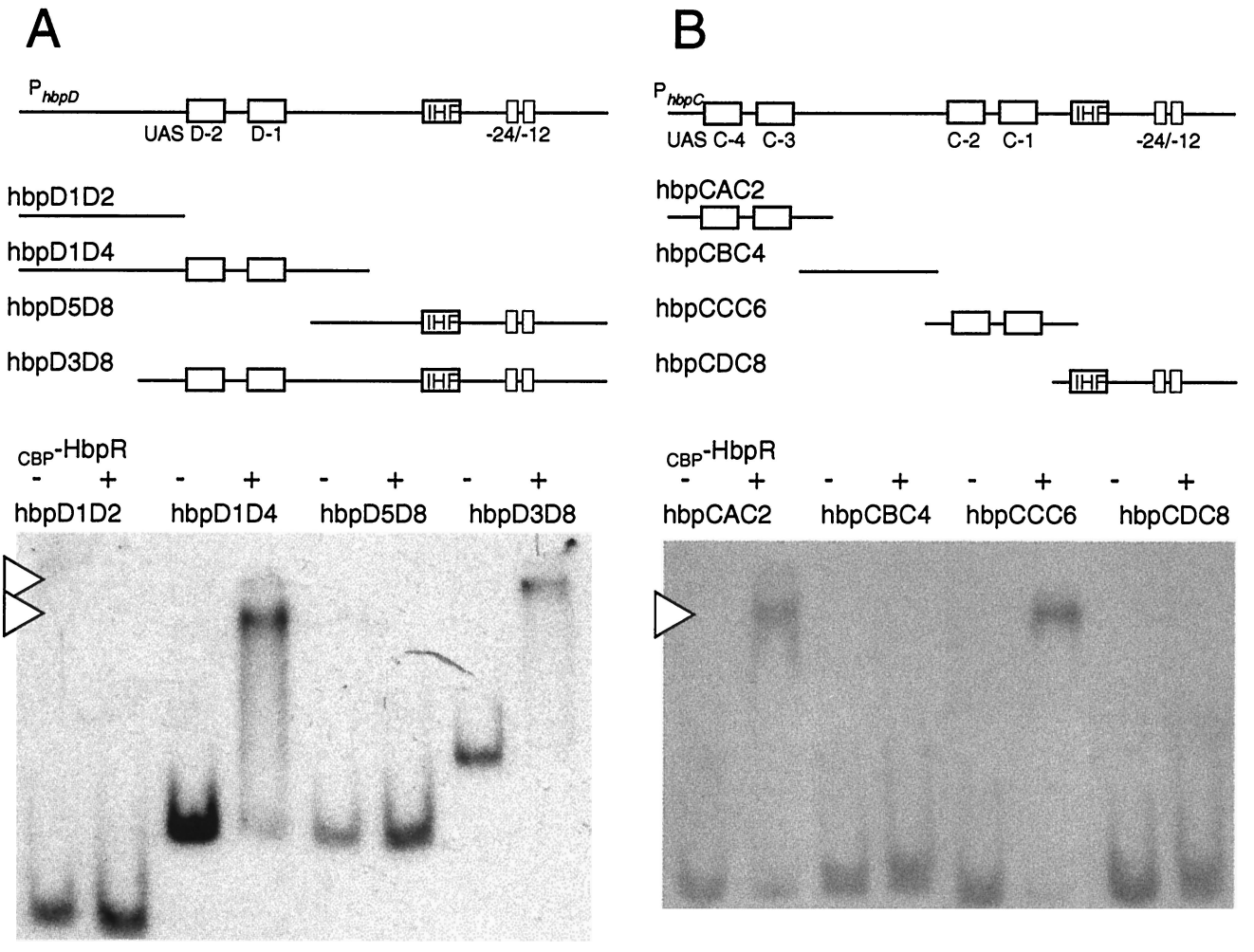

FIG. 3. CBP-HbpR binding to different fragments from P_{hbpD} and P_{hbpC}. (A) GMSA of P_{hbpD} fragments incubated with or without 1 μM CBP-HbpR (plus or minus at the top of the gel). The locations and relative sizes of the fragments are depicted in the diagram. Arrowheads indicate DNA-HbpR complexes. The name of the fragment corresponds to the primer name used in the PCR. (B) GMSA of P_{hbpC} fragments incubated with or without CBP-HbpR. Conditions and symbols are as described for panel A. IHF, integration host factor.

contained two HbpR binding sites, located between −604 to −468 and −256 to −140. These results confirmed the results of previous studies which had indicated that these regions act as sites for HbpR-mediated transcriptional activation (12).

CBP-HbpR simultaneously binds two palindromic sequences in its binding region. Previous promoter fusion studies and the GMSAs identified coarsely those regions on the DNA with which HbpR interacted. Sequence comparisons had suggested the presence within those regions of pairs of palindromic sequences which were similar to the so-called UASs of transcription activators of the XylR/DmpR type (11). To identify whether HbpR was indeed binding to these putative UASs, we performed DNase I footprinting analyses with CBP-HbpR and with labeled fragments containing UASs C-1 and C-2 (fragment hbpCCC6, within the *hbpC* promoter) or UASs D-1 and D-2 (fragment hbpD3D4, within the *hbpD* promoter). Both top and bottom strands of these fragments were subjected to DNase I nicking in the presence of increasing amounts of CBP-HbpR (Fig. 4 and 5). When the top-strand-labeled hbpCCC6 fragment was incubated with CBP-HbpR, protection appeared more or less at the predicted UASs, C-1 and C-2, or in directly neighboring nucleotides. The protection of these sites was confirmed by DNase I footprinting analysis of the bottom strand. The interaction of CBP-HbpR with the UASs became visible at concentrations of between 100 and 200 nM. Furthermore, no preferential or sequential protection of one or the other UAS was observed, suggesting that CBP-HbpR simultaneously binds to both UASs. As far as the resolution of the DNase I digestion pattern allowed, the base pairs contacted by CBP-HbpR within both UASs were very similar; basically, three regions within each UAS were protected, alternating with nonaffected base pairs and two neighboring hypersensitive base pairs (at positions −192 and −193 on the bottom strand) (Fig. 4). The protection pattern for the *hbpD* promoter fragment (hbpD3D4) (Fig. 5) was very similar to that for UASs C-1 and C-2. Both *hbpD* and *hbpC* promoters revealed a hypersensitive site located at the same base pair (TG) of both proximal UASs. The formation of hypersensitive sites probably reflected torsion of the DNA helix upon CBP-HbpR binding.

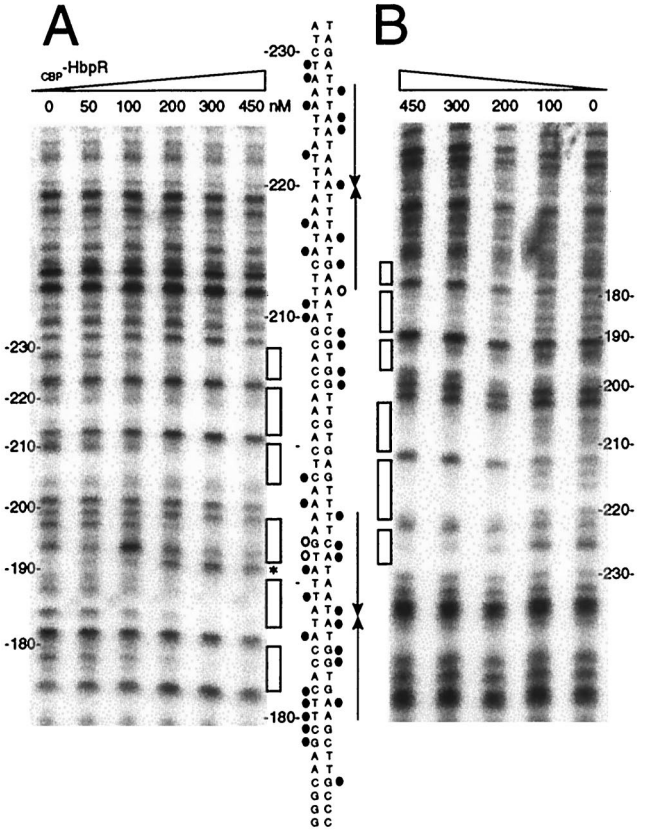

FIG. 4. DNase I footprinting analysis of CBP-HbpR binding to UASs C-1 and C-2. The 229-bp ^{32}P-end-labeled fragment hbpCCC6 containing UASs C-1 and C-2 was incubated with increasing amounts of CBP-HbpR (0 to 450 nM). (A) CBP-HbpR-mediated DNase I protection pattern for the bottom strand. (B) CBP-HbpR-mediated DNase I protection pattern for the top strand. Boxes indicate the regions protected from DNase I digestion upon the addition of CBP-HbpR. Between the panels, the sequences of UASs C-1 and C-2 and the positions that were contacted by CBP-HbpR are shown. Black circles indicate protection from DNase I digestion, while open circles and the asterisk indicate increased sensitivity to DNase I. The positions of the palindromes are indicated by arrows. Nucleotide numbering was relative to the transcriptional start site of *hbpC*.

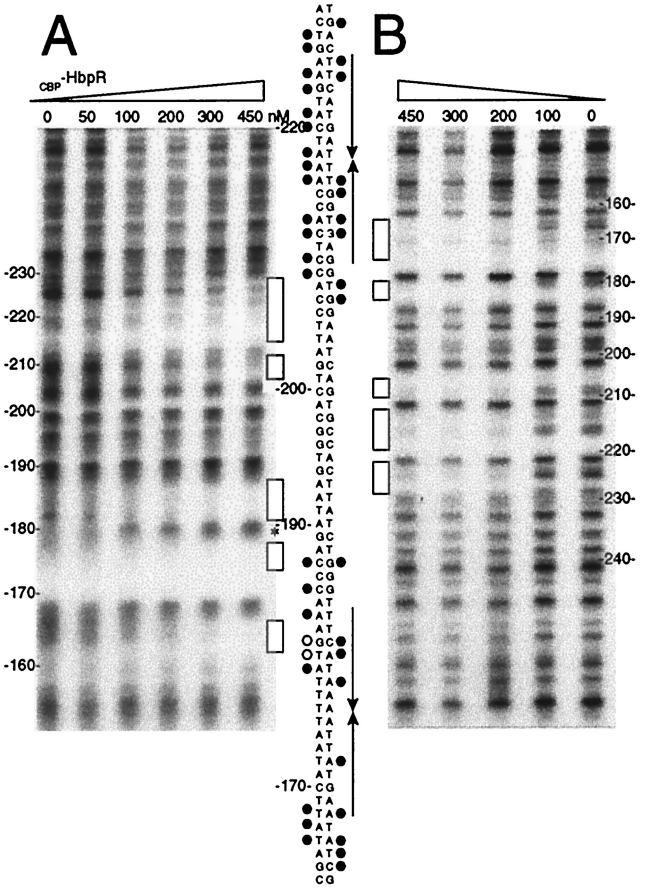

FIG. 5. DNase I footprinting analysis of CBP-HbpR binding to UASs D-1 and D-2. The 256-bp ^{32}P-end-labeled fragment hbpD3D4 containing UASs D-1 and D-2 was incubated with increasing amounts of CBP-HbpR (0 to 450 nM). (A) CBP-HbpR-mediated DNase I protection pattern for the bottom strand of hbpD3D4. (B) CBP-HbpR-mediated DNase I protection pattern for the top strand of hbpD3D4. Nucleotide numbering was relative to the *hbpD* transcriptional start site. For symbols and further explanations, see the legend to Fig. 4.

Affinity of CBP-HbpR for its binding sites. The affinity of CBP-HbpR for its three pairs of UASs in the *hbp* gene region was studied by GMSA titration. Increasing amounts of CBP-HbpR (between 0 and 600 nM) were allowed to contact DNA fragments with either UASs C-1 and C-2 (hbpCCC6) or UASs C-3 and C-4 (hbpCAC2) in the *hbpC* promoter or UASs D-1 and D-2 (hbpD3D4) in the *hbpD* promoter. In the presence of CBP-HbpR, two protein-DNA complexes were observed; one of these had not migrated into the gel at all (called complex 1), whereas the other had migrated to just below the wells (called complex 2) (Fig. 6A). Neither complex was present when the CBP-HbpRΔ purified fraction was incubated with the fragments containing each of the pairs of UASs (data not shown). This result indicated that the complexes were caused by HbpR-mediated binding. With increasing amounts of CBP-HbpR, the band corresponding to protein-DNA complex 2 increased in intensity (Fig. 6A), whereas the amount of complex 1 varied little. With laser densitometry, the relative densities of complex 2 obtained with increasing amounts of HbpR were calculated (Fig. 6B). Such affinity curves were made for all three pairs of UASs (Fig. 7B) and showed that CBP-HbpR had the highest affinity for UASs C-1 and C-2 (50% binding at 270 nM CBP-HbpR). Both UASs C-3 and C-4 and UASs D-1 and D-2 were bound with less affinity (50% binding at 430 and 490 nM CBP-HbpR, respectively). The reason for this affinity difference may lay in differences among the palindromic sequences which constitute the UASs or in the different amounts of spacing between the pairs of palindromic sequences.

Affinity of CBP-HbpR for UASs C-1 and C-2 changes in the presence of ATP and 2-HBP. When increasing concentrations of CBP-HbpR were incubated with UASs C-1 and C-2 in the presence of ATP and/or 2-HBP, the following changes in binding affinity were observed in GMSAs. When tested separately, ATP and 2-HBP did not significantly change the binding affinity of CBP-HbpR for UASs C-1 and C-2 (50% binding at 270 nM CBP-HbpR) (Fig. 6C). However, the addition of both ATP and 2-HBP resulted in the formation of a CBP-HbpR–DNA complex at lower CBP-HbpR concentrations (50% bind-

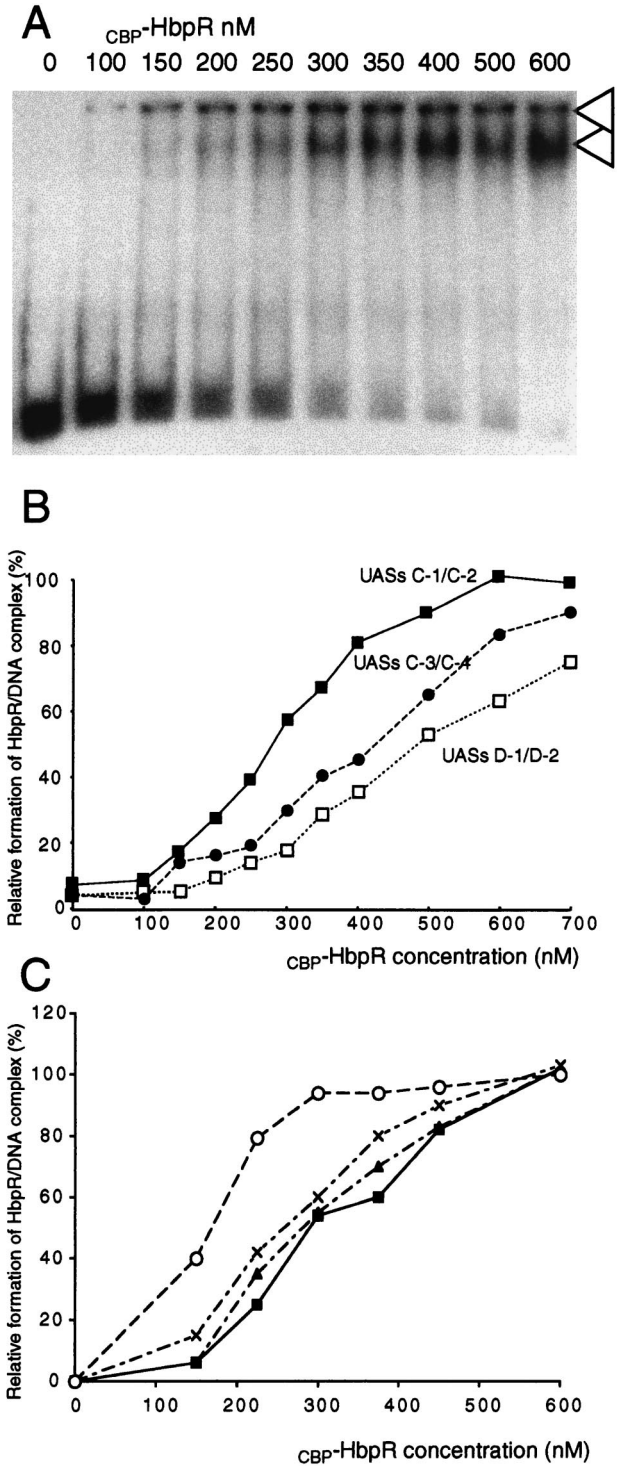

FIG. 6. Affinity characteristics of CBP-HbpR. (A) GMSA of fragment hbpCCC6 containing UASs C-1 and C-2 with increasing concentrations of CBP-HbpR (indicated above lanes). The amount of radiolabeled DNA fragment in the assay corresponded to 80 fmol. The arrowheads point to complex 1 (top) and complex 2 (bottom) (see text). (B) Graphic representation of the relative densities of the CBP-HbpR–DNA complexes formed with increasing CBP-HbpR concentrations with fragments containing UASs C-1 and C-2, UASs C-3 and C-4, and UASs D-1 and D-2. Relative densities were calculated by laser scanning densitometric analysis of band darkness on autoradiograms (as shown in panel A) and represent the darkness of the protein-DNA complex in each lane compared to that in the incubation with 600 nM HbpR. (C) Graphic representation of the relative densities of the CBP-HbpR–DNA complexes formed with increasing CBP-HbpR concentrations with fragments containing UASs C-1 and C-2 in the presence of ATP (multiplication signs), 2-HBP (triangles), and ATP and 2-HBP (open circles) or in the absence of an inducer (closed squares). ATP was used at a concentration of 5 mM, and 2-HBP was used at 10 μM. Relative densities were calculated as explained for panel B.

ing at 170 nM CBP-HbpR). The distances to which the CBP-HbpR–DNA complex migrated in the gel in the presence or absence of ATP and 2-HBP did not differ, suggesting that the compositions of the protein-DNA complexes were similar under all four tested conditions. Increased binding affinity of CBP-HbpR was optimal at 2-HBP concentrations of between 10 and 100 μM. At higher 2-HBP concentrations, the binding affinity of CBP-HbpR decreased and was fully abolished at 1 mM 2-HBP (data not shown). At high 2-HBP concentrations, the proteins may become denatured.

The presence and the conformation of the UASs C-1 and C-2 are critical for the binding of HbpR. We next addressed whether cooperative interactions were necessary for HbpR binding to UASs C-1 and C-2. We used GMSAs with fragments that contained either one or both pairs of palindromic sequences making up the UASs. Only the DNA fragment containing both UASs C-1 and C-2 was bound by CBP-HbpR (at 600 nM HbpR) (Fig. 7A). In contrast, DNA fragments containing only UAS C-1 or UAS C-2 were not bound by CBP-HbpR (Fig. 7A, lanes B and C). The addition of 2-HBP and ATP to assays with CBP-HbpR and DNA fragments with only UAS C-1 or UAS C-2 did not result in a stable protein-DNA complex visible on GMSAs either, not even at 600 nM CBP-HbpR (data not shown). These results demonstrated that both pairs of palindromes were needed for HbpR binding and suggested that some sort of cooperativity is needed between different HbpR protein complexes (most likely dimers bound to each UAS).

We next addressed whether the 32-bp spacing between the centers of UASs C-1 and C-2 is critical for cooperative interactions. We constructed fragments in which the intervening sequences between the two palindromes were increased by 5 and 10 bp (half helical and full helical insertions, respectively). Both the DNA with the original configuration and a DNA fragment with an additional 10 bp between the palindromes were completely bound in GMSAs at 600 nM CBP-HbpR (Fig. 7B, lanes A and B). However, the DNA fragment with an additional 5 bp between the palindromes did not form a stable protein-DNA complex at 600 nM CBP-HbpR. Rather, a smear was visible (Fig. 7B, lane C), suggesting that some binding by CBP-HbpR occurred but that the complex was not stable under the conditions of the gel analysis. Even at 1,200 nM, the DNA fragment was still not completely bound by CBP-HbpR. These results indicated that increasing the spacing between the palindromes by 5 bp (half helical insertion) destabilized the formation of the HbpR-DNA complex, whereas the insertion of 10 bp did not. Furthermore, these results showed that the affinity differences between UASs C-1 and C-2 and UASs D-1 and D-2 (with spacings of 32 and 42 bp between the centers of

the palindromes, respectively) were not necessarily caused by spacing differences between the pairs of palindromes.

DISCUSSION

It was previously shown that HbpR, the transcription activator for the 2-HBP pathway in *P. azelaica*, mediates transcription from two σ^{54}-dependent promoters, one of which is in front of the *hbpC* gene and the other of which is in front of the *hbpD* gene (11). HbpR has moderate sequence similarity to XylR but still belongs to the same subclass of the NtrC family of transcription activators (11). Here, we confirmed part of the working hypothesis for HbpR-mediated activation by showing the in vitro DNA binding of a partially purified CBP-HbpR fusion protein to promoter fragments. In addition, we discovered the binding of HbpR to a region (UASs C-3 and C-4) which does not function as a promoter for *hbp* transcription but which earlier had been noted as a potentially intact HbpR binding site (12). DNase I footprinting located the HbpR binding sites to two pairs of palindromic sequences which previously had been predicted as potential binding sites from DNA sequence comparisons with the XylR and DmpR binding sites (11). Unfortunately, we were not able to completely purify CBP-HbpR to homogeneity, nor were we able to cleave the CBP tag from HbpR without causing the loss of its activity. In principle, therefore, the presence of two other proteins in the fractions used for the DNA binding studies could have been responsible for the binding, and the CBP tag could have influenced the behavior of HbpR. From experiments in which we used purified protein extracts from *E. coli* producing CBP-HbpR with a large C-terminal deletion, we concluded that the contaminating proteins were not causing the observed DNA binding. Since the expression of the bacterial luciferase from P_{hbpC} in the presence of CBP-HbpR was similar to that in the native HbpR configuration, we concluded that the CBP tag also did not change the properties of the HbpR protein to activate the P_{hbpC} promoter. Furthermore, the CBP-HbpR fraction bound the *hbpRC* and *hbpAD* intergenic regions specifically, indicating that the CBP tag in the N-terminal part of HbpR did not disturb DNA binding. This notion is consistent with the finding that the N-terminal portions of the XylR and DmpR proteins did not affect DNA binding properties (19). In this respect, the 4-kDa CBP tag behaves in a manner similar to that of the 2-kDa His tag, which recently was used for purification of the XylR/DmpR-type transcription activator TouR (3).

In the absence of an effector and ATP, HbpR binds simultaneously to both pairs of UASs, a behavior similar to that of DmpR (34) but different from that of a constitutively active XylR variant devoid of the A domain (20). Furthermore, GMSAs with fragments with deletions of either UAS C-1 or UAS C-2 showed that one UAS was not sufficient for HbpR binding, not even in the presence of ATP and 2-HBP. This finding is consistent with initial observations made for the binding of NtrC from *Salmonella enterica* serovar Typhimurium (22) to the enhancer (UAS) in the *glnA* promoter (4, 24), although more recent studies demonstrated the binding of NtrC to an (artificial) single UAS (26, 31). The absence of binding to a single UAS suggests that HbpR binding is cooperative; i.e., the presence of the second UAS is needed to obtain full occupancy of both binding sites. Since we only observed one type of protein-DNA complex in GMSAs and DNA binding only with fragments containing both UASs, we presume that the complexes in GMSA consisted of two dimers

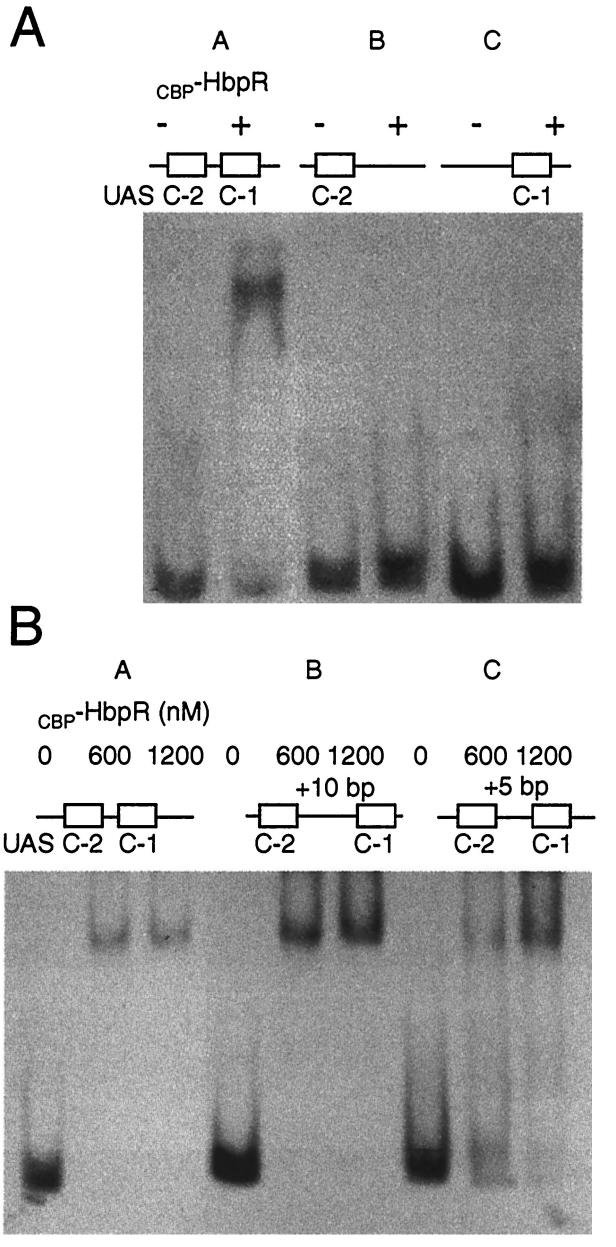

FIG. 7. GMSAs with fragments containing modified UASs C-1 and C-2 and CBP-HbpR. (A) Effect of deleting one UAS on the binding of CBP-HbpR. Lanes: A, incubation of DNA fragment hbpCCC6, containing the native configuration of UASs C-1 and C-2, with (+) or without (−) 600 nM CBP-HbpR; B, incubation with the insert of pHB156 containing only the proximal UAS, C-1; C, incubation with the insert of pHB157 containing only the distal UAS, C-2 (12). (B) Effect of adding 5 and 10 bp between the two palindromes comprising UASs C-1 and C-2. Lanes: A, incubation with fragment hbpCCC6; B, incubation with the insert of pHB163, containing the 10-bp insertion; C, incubation with the insert of pHB162, containing the 5-bp insertion. The amount of CBP-HbpR added to each binding assay mixture is indicated above each lane.

of HbpR occupying both UASs, as in the case of NtrC (26). Therefore, we were unable to identify which of the UASs is bound by HbpR with a greater affinity.

The cooperativity of HbpR binding was not affected by an additional 10 bp between the two binding sites. Inserting 10 bp would result in the two binding sites being separated although maintained on the same side of the helix. Apparently, however, the HbpR dimers binding to this region could still produce the normal protein-protein interactions required for cooperativity. In fact, the insertion of 10 bp resulted in a configuration of both UASs similar to the spacing between the two palindromes in the *hbpD* promoter. Therefore, wider spacing between the UASs cannot explain the weaker affinity of HbpR for P_{hbpD} than for P_{hbpC}. A 5-bp insertion, on the other hand, would diminish the binding of HbpR, probably by positioning the UASs on opposite sides of the DNA helix. In addition, for XylR and DmpR it was shown that offsetting the distal UAS relative to the proximal one lowered promoter activity (20, 34).

Essential components in the complete activation cycle of NtrC-type proteins are the activation of the protein and the formation of an oligomeric complex at the UASs, most likely consisting of a tetramer of dimers (26, 31). The binding affinity of phosphorylated NtrC for the enhancer is slightly greater than that for unphosphorylated NtrC (4, 26), a fact which could explain why activated HbpR (in the presence of 2-HBP and ATP) binds the UAS DNA fragment more efficiently than inactive HbpR. The observed apparent change in the binding affinity of activated CBP-HbpR for the UASs (i.e., in the presence of 2-HBP and ATP) is the first time that this finding has been reported for a protein of the XylR/DmpR subclass. Studies with XylR have mostly been hindered by the inability to purify the intact protein. For this reason, a constitutively active form of XylR devoid of its N-terminal effector binding domain has been used because it could be purified. However, some of the results with respect to the cooperativity of DNA binding by XylR therefore may have been slightly different from those obtained with the complete protein (7). For example, DctD variants devoid of the N-terminal portion are constitutively active, like XylR but different from NtrC (16). However, the magnitude of the cooperative binding of DctD to its UASs changed when the N-terminal portion was deleted (30). For the wild-type DctD protein, the intrinsic affinity was 20-fold lower for the distal binding site than for the proximal binding site; however, for the truncated, constitutively active protein, DctDΔ1-142 (with a deletion of the N-terminal portion), the affinity difference was larger (30). These findings demonstrate that deletion of a portion of the protein not directly involved in DNA binding can have an influence on its DNA binding properties. For NtrC, a different phenomenon was observed. A constitutively active mutant form of NtrC exists, although it has a single amino acid change (i.e., S160F). The NtrC-S160F protein had the same binding affinity for its UASs as the NtrC protein but demonstrated greater cooperativity, apparently due to new protein-protein contacts (31). Since DNA binding studies are possible with an intact HbpR protein, the HbpR system may be important in refining the model of activation by XylR/DmpR-type transcription activators.

The full activation cycle for NtrC-type and XylR/DmpR-type transcription activators probably is as follows. In solution, the proteins exist as dimers, as proven for NtrC (26); under nonactivating conditions, the proteins bind as a pair of dimers to their enhancer (UASs) (26). In this form, NtrC has low ATPase activity (35), and it is assumed that no proper contacts can be formed between NtrC and σ^{54} RNA polymerase complexed to the promoter. Upon phosphorylation, NtrC changes affinity for its binding site and forms a larger complex at the UASs (most likely octamers) (26, 31). NtrC subunits inside this complex may have increased ATPase activity, and the complex itself will interact with the σ^{54} RNA polymerase-promoter complex, resulting in transcriptional initiation. For XylR, it has been proposed that in the presence of ATP, the protein-DNA structures seem to constantly assemble and disassemble between octamers and two dimer pairs (7). This scenario could explain why no higher-order structures of activated HbpR and the UAS C-1 and C-2 fragments were visible in GMSAs, as the equilibrium was mostly on the side of the dimer pair interaction.

REFERENCES

1. **Abril, M. A., M. Buck, and J. L. Ramos.** 1991. Activation of the *Pseudomonas* TOL plasmid upper pathway operon. J. Biol. Chem. **266:**15832–15838.
2. **Abril, M. A., and J. L. Ramos.** 1993. Physical organization of the upper pathway operon promoter of the *Pseudomonas* TOL plasmid. Sequence and positional requirements for XylR-dependent activation of transcription. Mol. Gen. Genet. **239:**281–288.
3. **Arenghi, F. L., P. Barbieri, G. Bertoni, and V. de Lorenzo.** 2001. New insights into the activation of *o*-xylene biodegradation in *Pseudomonas stutzeri* OX1 by pathway substrates. EMBO Rep. **2:**409–414.
4. **Chen, P., and L. J. Reitzer.** 1995. Active contribution of two domains to cooperative DNA binding of the enhancer-binding protein nitrogen regulator I (NtrC) of *Escherichia coli*: stimulation by phosphorylation and the binding of ATP. J. Bacteriol. **177:**2490–2496.
5. **de Lorenzo, V., M. Herrero, M. Metzke, and K. N. Timmis.** 1991. An upstream XylR- and IHF-induced nucleoprotein complex regulates the σ^{54}-dependent P *u* promoter of TOL plasmid. EMBO J. **10:**1159–1167.
6. **Dixon, R.** 1986. The *xylABC* promoter from the *Pseudomonas putida* TOL plasmid is activated by nitrogen regulatory genes in *Escherichia coli*. Mol. Gen. Genet. **203:**129–136.
7. **Garmendia, J., and V. de Lorenzo.** 2000. Visualization of DNA-protein intermediates during activation of the P *u* promoter of the TOL plasmid of *Pseudomonas putida*. Microbiology **146:**2555–2563.
8. **Gomada, M., S. Inouye, H. Imaishi, A. Nakazawa, and T. Nakazawa.** 1992. Analysis of an upstream regulatory sequence required for activation of the regulatory gene *xylS* in xylene metabolism directed by the TOL plasmid of *Pseudomonas putida*. Mol. Gen. Genet. **233:**419–426.
9. **Inouye, S., M. Gomada, U. M. X. Sangodkar, A. Nakazawa, and T. Nakazawa.** 1990. Upstream regulatory sequence for transcriptional activator XylR in the first operon of xylene metabolism on the TOL plasmid. J. Mol. Biol. **216:**251–260.
10. **Inouye, S., A. Nakazawa, and T. Nakazawa.** 1988. Nucleotide sequence of the regulatory gene *xylR* of the TOL plasmid from *Pseudomonas putida*. Gene **66:**301–306.
11. **Jaspers, M. C., A. Schmid, M. H. Sturme, D. A. Goslings, H. P. Kohler, and J. R. Van Der Meer.** 2001. Transcriptional organization and dynamic expression of the *hbpCAD* genes, which encode the first three enzymes for 2-hydroxybiphenyl degradation in *Pseudomonas azelaica* HBP1. J. Bacteriol. **183:** 270–279.
12. **Jaspers, M. C., M. Sturme, and J. R. van Der Meer.** 2001. Unusual location of two nearby pairs of upstream activating sequences for HbpR, the main regulatory protein for the 2-hydroxybiphenyl degradation pathway of *'Pseudomonas azelaica '* HBP1. Microbiology **147:**2183–2194.
13. **Jaspers, M. C., W. A. Suske, A. Schmid, D. A. Goslings, H. P. Kohler, and J. R. van der Meer.** 2000. HbpR, a new member of the XylR/DmpR subclass within the NtrC family of bacterial transcriptional activators, regulates expression of 2-hydroxybiphenyl metabolism in *Pseudomonas azelaica* HBP1. J. Bacteriol. **182:**405–417.
14. **Kohler, H. P. E., D. Kohler-Staub, and D. D. Focht.** 1988. Degradation of 2-hydroxybiphenyl and 2,2′-dihydroxybiphenyl by *Pseudomonas* sp. strain HBP1. Appl. Environ. Microbiol. **54:**2683–2688.
15. **Kohler, H. P. E., A. Schmid, and M. van der Maarel.** 1993. Metabolism of 2,2′-dihydroxybiphenyl by *Pseudomonas* sp. strain HBP1: production and consumption of 2,2′,3-trihydroxybiphenyl. J. Bacteriol. **175:**1621–1628.
16. **Lee, J. H., D. Scholl, B. T. Nixon, and T. R. Hoover.** 1994. Constitutive ATP hydrolysis and transcription activation by a stable, truncated form of *Rhizobium meliloti* DCTD, a σ^{54}-dependent transcriptional activator. J. Biol. Chem. **269:**20401–20409.

17. **Morett, E., and L. Segovia.** 1993. The σ^{54} bacterial enhancer-binding protein family: mechanism of action and phylogenetic relationship of their functional domains. J. Bacteriol. **175:**6067–6074.
18. **Pérez-Martín, J., and V. de Lorenzo.** 1996. ATP binding to the σ^{54}-dependent activator XylR triggers a protein multimerization cycle catalyzed by UAS DNA. Cell **86:**331–339.
19. **Pérez-Martín, J., and V. de Lorenzo.** 1996. *In vitro* activities of an N-terminal truncated form of XylR, a σ^{54}-dependent transcriptional activator of *Pseudomonas putida*. J. Mol. Biol. **258:**575–587.
20. **Pérez-Martín, J., and V. de Lorenzo.** 1996. Physical and functional analysis of the prokaryotic enhancer of the σ^{54}-promoters of the TOL plasmid of *Pseudomonas putida*. J. Mol. Biol. **258:**562–574.
21. **Pérez-Martín, J., F. Rojo, and V. de Lorenzo.** 1994. Promoters responsive to DNA bending: a common theme in prokaryotic gene expression. Microbiol. Rev. **58:**268–290.
22. **Porter, S. C., A. K. North, A. B. Wedel, and S. Kustu.** 1993. Oligomerization of NtrC at the *glnA* enhancer is required for transcriptional activation. Genes Dev. **7:**2258–2273.
23. **Ravatn, R., S. Studer, A. J. B. Zehnder, and J. R. van der Meer.** 1998. Int-B13, an unusual site-specific recombinase of the bacteriophage P4 integrase family, is responsible for chromosomal insertion of the 105-kilobase *clc* element of *Pseudomonas* sp. strain B13. J. Bacteriol. **180:**5505–5514.
24. **Reitzer, L. J., and B. Magasanik.** 1986. Transcription of *glnA* in *E. coli* is stimulated by activator bound to sites far from the promoter. Cell **45:**785–792.
25. **Rippe, K.** 2000. Simultaneous binding of two DNA duplexes to the NtrC-enhancer complex studied by two-color fluorescence cross-correlation spectroscopy. Biochemistry **39:**2131–2139.
26. **Rippe, K., N. Mucke, and A. Schulz.** 1998. Association states of the transcription activator protein NtrC from *E. coli* determined by analytical ultracentrifugation. J. Mol. Biol. **278:**915–933.
27. **Sambrook, J., E. F. Fritsch, and T. Maniatis.** 1989. Molecular cloning: a laboratory manual, 2nd ed. Cold Spring Harbor Laboratory Press, Cold Spring Harbor, N.Y.
28. **Sanger, F., S. Nicklen, and A. R. Coulson.** 1977. DNA sequencing with chain-terminating inhibitors. Proc. Natl. Acad. Sci. USA **74:**5463–5467.
29. **Schmid, A.** 1997. Ph.D. thesis. Universität Stuttgart, Stuttgart, Germany.
30. **Scholl, D., and B. T. Nixon.** 1996. Cooperative binding of DctD to the dctA upstream activation sequence of Rhizobium meliloti is enhanced in a constitutively active truncated mutant. J. Biol. Chem. **271:**26435–26442.
31. **Sevenich, F. W., J. Langowski, V. Weiss, and K. Rippe.** 1998. DNA binding and oligomerization of NtrC studied by fluorescence anisotropy and fluorescence correlation spectroscopy. Nucleic Acids Res. **26:**1373–1381.
32. **Shingler, V.** 1996. Signal sensing by σ^{54}-dependent regulators: derepression as a control mechanism. Mol. Microbiol. **19:**409–416.
33. **Sticher, P., M. C. M. Jaspers, K. Stemmler, H. Harms, A. J. B. Zehnder, and J. R. van der Meer.** 1997. Development and characterization of a whole-cell bioluminescent sensor for bioavailable middle-chain alkanes in contaminated groundwater samples. Appl. Environ. Microbiol. **63:**4053–4060.
34. **Sze, C. C., A. D. Laurie, and V. Shingler.** 2001. In vivo and in vitro effects of integration host factor at the DmpR-regulated σ^{54}-dependent Po promoter. J. Bacteriol. **183:**2842–2851.
35. **Weiss, D. S., J. Batut, K. E. Klose, J. Keener, and S. Kustu.** 1991. The phosphorylated form of the enhancer-binding protein NTRC has an ATPase activity that is essential for activation of transcription. Cell **67:**155–167.
36. **Wyborski, D. L., J. C. Bauer, C. F. Zheng, K. Felts, and P. Vaillancourt.** 1999. An *Escherichia coli* expression vector that allows recovery of proteins with native N-termini from purified calmodulin-binding peptide fusions. Protein Expr. Purif. **16:**1–10.
37. **Wyman, C., I. Rombel, A. K. North, C. Bustamante, and S. Kustu.** 1997. Unusual oligomerization required for activity of NtrC, a bacterial enhancer-binding protein. Science **275:**1658–1661.